Hydrogen Atom Transfer Reactions of a Ruthenium Imidazole Complex: Hydrogen Tunneling and the Applicability of the Marcus Cross Relation

Adam Wu and **James M. Mayer**[*]
Department of Chemistry, University of Washington, Campus Box 351700, Seattle, WA, 98195-1700, USA

Abstract

The reaction of $Ru^{II}(acac)_2(py\text{-}imH)$ (**$Ru^{II}imH$**) with TEMPO$^\bullet$ (2,2,6,6-tetramethyl-piperidine-1-oxyl radical) in MeCN quantitatively gives $Ru^{III}(acac)_2(py\text{-}im)$ (**$Ru^{III}im$**) and the hydroxylamine TEMPO-H by transfer of H$^\bullet$ ($H^+ + e^-$) (acac = 2,4-pentanedionato, py-imH = 2-(2′-pyridyl) imidazole). Kinetic measurements of this reaction by UV-vis stopped-flow techniques indicate a bimolecular rate constant $k_{3H} = 1400 \pm 100$ M^{-1} s^{-1} at 298 K. The reaction proceeds via a concerted hydrogen atom transfer (HAT) mechanism, as shown by ruling out the stepwise pathways of initial proton or electron transfer due to their very unfavorable thermochemistry ($\Delta G°$). Deuterium transfer from $Ru^{II}(acac)_2(py\text{-}imD)$ (**$Ru^{II}imD$**) to TEMPO$^\bullet$ is surprisingly much slower at $k_{3D} = 60 \pm 7$ M^{-1} s^{-1}, with $k_{3H}/k_{3D} = 23 \pm 3$ at 298 K. Temperature dependent measurements of this deuterium kinetic isotope effect (KIE) show a large difference between the apparent activation energies, $E_{a3D} - E_{a3H} = 1.9 \pm 0.8$ kcal mol^{-1}. The large k_{3H}/k_{3D} and ΔE_a values appear to be greater than the semi-classical limits and thus suggest a tunneling mechanism. The self-exchange HAT reaction between **$Ru^{II}imH$** and **$Ru^{III}im$**, measured by ^{1}H NMR line broadening, occurs with $k_{4H} = (3.2 \pm 0.3) \times 10^5$ M^{-1} s^{-1} at 298 K and $k_{4H}/k_{4D} = 1.5 \pm 0.2$. Despite the small KIE, tunneling is suggested by the ratio of Arrhenius pre-exponential factors, $\log(A_{4H}/A_{4D}) = -0.5 \pm 0.3$. These data provide a test of the applicability of the Marcus cross relation for H and D transfers, over a range of temperatures, for a reaction that involves substantial tunneling. The cross relation calculates rate constants for **$Ru^{II}imH$** (**D**) + TEMPO$^\bullet$ that are greater than those observed: $k_{3H,calc}/k_{3H} = 31 \pm 4$ and $k_{3D,calc}/k_{3D} = 140 \pm 20$ at 298 K. In these rate constants and in the activation parameters, there is a better agreement with the Marcus cross relation for H than for D transfer, despite the greater prevalence of tunneling for H. The cross relation does not explicitly include tunneling, so close agreement should not be expected. In light of these results, the strengths and weaknesses of applying the cross relation to HAT reactions are discussed.

Introduction

Hydrogen atom transfer (HAT) – the transfer of a H$^\bullet$ ($H^+ + e^-$) from one reagent to another in a single kinetic step – is important in many chemical and biological processes.[1–6] Examples include reactions of alkoxyl,[7] nitroxyl[8] and other radicals, peroxidation of poly-unsaturated fatty acids by lipoxygenases,[9] hydrocarbon oxidation by oxo-metal complexes,[10] and terephthalic acid manufacture from *p*-xylene.[11] The involvement of transition metal ions in many of these processes has broadened the traditional view of HAT, which is now viewed as one subset of proton-coupled electron transfer (PCET) processes.[12–14]

---
[*]To whom correspondence should be addressed. E-mail: mayer@chem.washington.edu.

Rate constants of organic HAT reactions have traditionally been analyzed using the Evans-Polanyi correlation with enthalpic driving force and bond dissociation enthalpies.[15] Our studies of transition metal reactions have shown that analyses of HAT processes should use free energies[16] and that the Marcus cross relation (eq 1) gives reasonably accurate predictions in

$$k_{XY} = \sqrt{k_{XX} k_{YY} K_{XY} f_{XY}}$$

(1)

many cases[17,18] (even though it was originally developed for electron transfer[19]). The cross rate constant (k_{XY}) is calculated from the self-exchange rate constants (k_{XX} and k_{YY}, eq 2), equilibrium constant (K_{XY}), and a factor f_{XY}.[19,20] The cross relation holds well for a number of reactions of

$$X^\bullet + HX \xrightarrow{k_{XX}} XH + X^\bullet$$

(2)

iron–tris(α-diimine) complexes, including the unusual inverse temperature dependence for the HAT reaction of $[Fe^{II}(H_2bip)_3]^{2+}$ with TEMPO$^\bullet$ (H$_2$bip = 2,2′-bi-1,4,5,6-tetrahydropyrimidine).[18] The cross relation has also been found to give good predictions – within one to two orders of magnitude – for some purely organic reactions[17] and for reactions of ruthenium and vanadium-oxo compounds.[21] However, larger deviations from the predictions of eq 1 have been found for osmium-anilido compounds[22] and other systems.[17,23,24] Modern theoretical treatments of HAT and PCET are much more sophisticated, including non-adiabatic effects, hydrogen tunneling, and involvement of vibrational excited states.[25] They do not simply reduce to the cross relation. Bridging the gap between experimental systems and theoretical treatments is not simple because many of the parameters in the theories are not experimentally accessible.[26]

This report describes what is perhaps the first comprehensive dataset for an HAT reaction: measurements of cross and self-exchange rate constants and equilibrium constants for both H and D as a function of temperature. To obtain such a dataset, we chose ruthenium complexes because of their substitution inertness and the accessibility of the Ru^{II} and Ru^{III} oxidation states. Complexes with a 2-(2′-pyridyl)imidazole (py-imH) ligand and two acac (2,4-pentanedionato) ligands have been prepared, and have the advantages of a single ionizable proton and accessible redox potentials.[27] Ru^{II}(acac)$_2$(py-imH) (**Ru^{II}imH**) undergoes clean hydrogen atom transfer to excess TEMPO$^\bullet$ (transferring one proton and one electron) to give Ru^{III}(acac)$_2$(py-im) (**Ru^{III}im**) and TEMPO-H (eq 3),[27] making this reaction appropriate for HAT
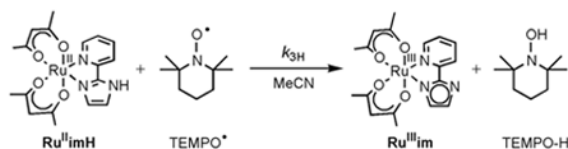
(3)

studies and Marcus analysis. The deuterium transfer from Ru^{II}(acac)$_2$(py-imD) (**Ru^{II}imD**) to TEMPO$^\bullet$ is much slower, with a large deuterium kinetic isotope effect (KIE), $k_{3H}/k_{3D} = 23 \pm$

3 at 298 K. As discussed below, this and other results indicate that hydrogen tunneling is occurring. Tunneling is also implicated in the HAT self-exchange between **Ru^{II}imH** and **Ru^{III}im**. Tunneling has come to be viewed as a seminal feature of hydrogen transfer reactions, from catalysis to laboratory reactions to enzymatic processes.[1] HAT from a fatty-acid substrate to the Fe^{III}OH active site in lipoxygenase enzymes, for instance, exhibits large k_H/k_D values of up to ~80.[9] In light of the data reported here for ruthenium HAT reactions and the involvement of tunneling, the applicability of the Marcus cross relation is discussed.

Results

I. Equilibrium Constant Measurements

The reaction of **Ru^{II}imH** with 1 equiv of TEMPO$^\bullet$ in CD$_3$CN at room temperature under N$_2$ rapidly yields **Ru^{III}im** and TEMPO-H (eq 3), as observed by ^{1}H NMR and UV-vis spectroscopies.[27] The equilibrium constant K_{3H} was determined by titrating a MeCN solution of **Ru^{III}im** (0.48 mM) with TEMPO-H (0.096–3.3 mM) in the reverse, uphill direction. Using the known ε values,[27] the optical spectra give the equilibrium concentrations of **Ru^{II}imH** and **Ru^{III}im**. A plot of [**Ru^{II}imH**][TEMPO$^\bullet$]/[**Ru^{III}im**] *vs.* [TEMPO-H] (Figure 1a) is linear with a slope of $1/K_{3H}$, yielding $K_{3H} = (1.8 \pm 0.2) \times 10^3$ at 298 K and $\Delta G°_{3H} = -4.4 \pm 0.1$ kcal mol^{-1}. This is in excellent agreement with the $\Delta G°_{3H}$ of -4.5 ± 0.9 kcal mol^{-1} derived from the difference in bond dissociation free energies (ΔBDFE) of **Ru^{II}imH** and TEMPO-H, as determined from electrochemical and pK_a measurements.[27] The equilibrium constant for deuterium atom transfer in eq 3 was determined analogously to be $K_{3D} = (2.5 \pm 0.3) \times 10^3$ ($\Delta G°_{3D} = -4.6 \pm 0.1$ kcal mol^{-1}), indicating an inverse equilibrium isotope effect of $K_{3H}/K_{3D} = 0.72 \pm 0.12$ at 298 K. An inverse isotope effect is expected because reaction 3 converts a lower-frequency N–H bond into a higher-frequency O–H bond. Using measurements of ν_{NH} and ν_{ND} in **Ru^{II}imH(D)** (KBr pellets) and ν_{OH} and ν_{OD} in TEMPO-H(D) (MeCN solution), $K_H/K_D = 0.78$ is calculated from a simple one-dimensional oscillator model.[28,29] van't Hoff analysis of K_{3H} and K_{3D} values from 269–310 K gives $\Delta H°_{3H} = -3.0 \pm 0.3$ kcal mol^{-1} and $\Delta S°_{3H} = 4.9 \pm 1.1$ cal mol^{-1} K^{-1}, and $\Delta H°_{3D} = -3.8 \pm 0.4$ kcal mol^{-1} and $\Delta S°_{3D} = 2.8 \pm 1.5$ cal mol^{-1} K^{-1} (Figure 1b).[30]

II. Kinetic Measurements

The kinetics for the HAT reaction of **Ru^{II}imH** (0.047–0.053 mM) with TEMPO$^\bullet$ (0.53–6.7 mM) in MeCN at 298 K have been determined under pseudo-first order conditions (>10 equiv of TEMPO$^\bullet$ using stopped-flow optical measurements in the visible region). **Ru^{II}imH** (λ_{max} = 568 nm, ε = 7000 M^{-1} cm^{-1}) converts to **Ru^{III}im** (λ_{max} = 486 nm, ε = 1600 M^{-1} cm^{-1}) in 90 ± 10% yield (Figure 2a); the absorbances of TEMPO$^\bullet$ and TEMPO-H are negligible in the observed spectral region at these concentrations. Global analysis of the spectra (460–660 nm) using SPECFIT software[31] showed a good fit to a simple first order A → B model (Figure 2b), indicating that the rate is first order in [**Ru^{II}imH**]. Plotting the derived pseudo-first order k_{obs} *vs.* the concentration of TEMPO$^\bullet$ yields a straight line (Figure 3a), showing that the rate is also first order in [TEMPO$^\bullet$], and yields the bimolecular rate constant, $k_{3H} = 1400 \pm 100$ M^{-1} s^{-1}.

The addition of CD$_3$OD to a solution of **Ru^{II}imH** in CD$_3$CN rapidly exchanges the imidazole N*H* to form Ru^{II}(acac)$_2$(py-imD) (**Ru^{II}imD**), so that the δ 11.3 N*H* resonance does not appear in the ^{1}H NMR spectrum. **Ru^{II}imD** was therefore prepared *in situ* in the presence of >400 equiv CD$_3$OD (99.8% D from Cambridge Isotope Laboratories) in MeCN. The kinetics for **Ru^{II}imD** (0.047–0.053 mM) plus excess TEMPO$^\bullet$ (0.53–75 mM) in MeCN (with 25 mM CD$_3$OD) at 298 K were measured as above to give $k_{3D} = 60 \pm 7$ M^{-1} s^{-1} (Figure 3a). Thus, there is a large deuterium KIE of $k_{3H}/k_{3D} = 23 \pm 3$ at 298 K. Measurements of k_{3H} and k_{3D} from 282–337 K (Figure 3b) give the Eyring and Arrhenius parameters shown in Table 1. The

presence of 25 mM CH$_3$OH does not affect the rate constants or activation parameters for **Ru^{II}imH** and TEMPO$^{\bullet}$ (Figure 3a), ruling out the presence of methanol as the cause of the much slower k_{3D}.

III. Self-Exchange Reactions of Ru^{II}imH(D) plus Ru^{III}im

The diamagnetic ^{1}H NMR resonances of **Ru^{II}imH** (2.0 mM) in CD$_3$CN broaden upon addition of small amounts of **Ru^{III}im** (0.092–0.73 mM), indicating exchange (self-exchange) between the two complexes (Figure 4, eq 4). The peaks broaden but do not shift, indicating that the NMR dynamics are in the slow-exchange limit.[33] The line width (fwhm) of the δ1.51 methyl resonance of **Ru^{II}imH** in CD$_3$CN was determined by Lorentzian line fitting using NUTS software.[34,35] A plot of $\pi(\Delta$fwhm) *vs.* [**Ru^{III}im**] yields a straight line (Figure 5a), with a slope equal to the self-exchange rate constant,
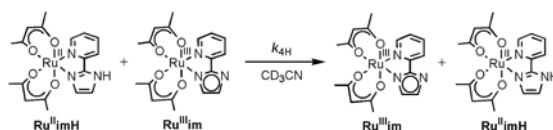
(4)

$k_{4H} = (3.2 \pm 0.3) \times 10^5$ M^{-1} s^{-1} at 298 K. The linewidths of the two overlapping CH-acac singlets (δ5.29, 5.32) and the pyridine doublet at δ8.75 were fitted (less precisely) using gNMR, [36] and analysis of their broadening gave the same rate constant as above within error. The broadening is uniform and proportional to the concentration of **Ru^{III}im**, which indicates that it is due to the self-exchange reaction. The deuterium self-exchange rate constant, **Ru^{II}imD** + **Ru^{III}im** in CD$_3$CN with 250 mM CD$_3$OD was measured analogously to be $k_{4D} = (2.1 \pm 0.2) \times 10^5$ M^{-1} s^{-1} (Figure 5a), so $k_{4H}/k_{4D} = 1.5 \pm 0.2$ at 298 K. Activation parameters for the H and D self-exchange, determined from rate constants from 250–363 K (Figure 5b), are given in Table 1 and discussed below. As for reaction 3, the presence of 250 mM CH$_3$OH did not affect the protio rate constant or activation parameters within error (Figures 5a and 5b).

The mechanism of net H-atom self exchange could be concerted HAT or transfer of the electron and proton in two separate steps, as discussed below. As part of this mechanistic analysis, we have investigated the effect of solvent and of added base. The line broadening observed in a solution of **Ru^{II}imH** (2.0 mM) and **Ru^{III}im** (0.040 mM) in CD$_3$CN is unaffected by the addition of Et$_3$N (0.020–0.10 mM). Since the rate of HAT self-exchange is unaffected by base, catalysis by trace acid[22] is not occurring. The self-exchange rate constant k_{4H} was also measured in THF-d_8 and found to be an order of magnitude faster than in CD$_3$CN, $(3.4 \pm 1.0) \times 10^6$ M^{-1} s^{-1} at 298 K. In these experiments, the initial resonances of **Ru^{II}imH** were quite broad (for the methyl signal at δ1.48, fwhm = 16 Hz), indicating the presence of a trace amount of **Ru^{III}imH$^+$** and/or **Ru^{III}im**. Adding a small amount of Cp$_2$Co (0.011 mM) sharpened the signal to 5 Hz, by reduction of any Ru^{III} species. This solution gave the same measured self-exchange rate constant k_{4H} within error as the solution without Cp$_2$Co pretreatment, similarly indicating that catalysis by trace oxidized impurities is not occurring.

Discussion

The **Ru^{II}imH**/**Ru^{III}im** system provides a unique opportunity to examine cross and self-exchange hydrogen and deuterium atom transfer reactions as a function of temperature. We first discuss the cross reaction of **Ru^{II}imH** + TEMPO$^{\bullet}$ and its mechanism, then the self-exchange reaction and its pathway. The results are then used to discuss the applicability of the

Marcus cross relation for HAT reactions, particularly for reactions involving significant tunneling.

I. HAT Reaction of $Ru^{II}imH(D)$ plus $TEMPO^{\bullet}$

A. Mechanism—The reaction of $\mathbf{Ru^{II}imH}$ + $TEMPO^{\bullet}$ → $\mathbf{Ru^{III}im}$ + TEMPO-H in MeCN (eq 3) could proceed through three possible pathways.[4a] It could proceed via (*i*) initial electron transfer (ET) forming $[Ru^{III}(acac)_2(py-imH)]^+$ ($\mathbf{Ru^{III}imH^+}$) and $TEMPO^-$ intermediates, (*ii*) initial proton transfer (PT) forming $[Ru^{II}(acac)_2(py-im)]^-$ ($\mathbf{Ru^{II}im^-}$) and $TEMPO\text{-}H^{+\bullet}$, or (*iii*) concerted HAT in a single kinetic step. The free energy changes for these three initial steps (Chart 1) can be calculated using the known thermochemistry of the ruthenium complexes[27] and $TEMPO^{\bullet}$/TEMPO-H in MeCN.[37] These ground state energies, which are the minimum values of the free energies of activation $\Delta G^{\ddagger}$, rule out the initial ET and initial PT pathways because they are much larger than the measured barrier, $\Delta G^{\ddagger}_{3H} = +13$ kcal mol^{-1} at 298 K. Thus reaction 3 must proceed by HAT, with $\Delta G^{\circ}_{3H} = -4.4$ kcal mol^{-1}. Similar arguments apply to the deuterium reaction. The unfavorable energetics of the ET and PT pathways are predominately due to high energy of the intermediates $TEMPO\text{-}H^{+\bullet}$ (very acidic, $pK_a \approx -3$) and $TEMPO^-$ (very reducing, $E^{\circ} \approx -1.9$ V *vs.* $Cp_2Fe^{+/0}$).[37] This kind of thermochemical analysis has been used to establish HAT mechanisms for a variety of reactions.[4–6,12a,13,17–21,38]

B. Tunneling—In the one dimensional semi-classical transition state limit, the $\Delta G^{\ddagger}_D - \Delta G^{\ddagger}_H$ for a reaction is at most the difference in zero-point energies. The large observed $k_{3H}/k_{3D} = 23 \pm 3$ at 298 K for reaction 3 is significantly greater than this semi-classical limit, $k_H/k_D = 6.9$ (calculated from $\nu_{NH}/\nu_{ND} = 3068/2267$ cm^{-1} of $\mathbf{Ru^{II}imH(D)}$).[39,40] Taking into account other vibrational modes, the observed k_{3H}/k_{3D} is still twice as large as Bell's estimate of the maximum semi-classical $k_H/k_D \approx 11$ for reaction of an O–H bond at 298 K.[39] Bell also proposed that tunneling is indicated when $E_{aD} - E_{aH}$ ($= \Delta H^{\ddagger}_D - \Delta H^{\ddagger}_H$) is larger than the difference in zero-point energies (1.1 kcal mol^{-1} for $\mathbf{Ru^{II}imH}$ *vs.* $\mathbf{Ru^{II}imD}$) and/or when the ratio of the protio and deutero pre-exponential factors deviate from unity: $|\log(A_H/A_D)| > 0.15$ ($A_H/A_D < 0.7$ or $A_H/A_D > 1.4$).[39] For reaction 3, the $E_{a3D} - E_{a3H}$ of 1.9 ± 0.8 kcal mol^{-1} appears to be greater than the semi-classical limit, while $\log(A_{3H}/A_{3D}) = 0.0 \pm 0.5$ is within the limit. The k_{3H}/k_{3D} and $E_{a3D} - E_{a3H}$ together indicate that hydrogen tunneling plays a significant role in this reaction.

Insight about the nature of the tunneling can be derived from the activation parameters using a model that considered four temperature regimes, as suggested by Klinman.[41] In the high-temperature limit (region I), the reaction proceeds classically, without tunneling, and $E_{aD} - E_{aH}$ and A_H/A_D are within the semi-classical limits. At somewhat lower temperatures (region II), hydrogen tunneling becomes significant (smaller E_{aH} and A_H) but D predominantly transfers over the barrier, so $E_{aD} - E_{aH}$ is large and $A_H \ll A_D$ [$\log(A_H/A_D) < 0$]. At the low-temperature limit (region IV), both hydrogen and deuterium tunnel extensively so that $E_{aD} - E_{aH}$ is small and $A_H \gg A_D$ [$\log(A_H/A_D) > 0$]. Since A_H is less than A_D in the limited tunneling region (II) but greater than A_D in the extensive tunneling regime (IV), there must be a crossover region (III) in which $E_{aD} - E_{aH}$ is still larger than the semiclassical value, but $A_H \approx A_D$ [$\log(A_H/A_D) \approx 0$]. For reaction 3, the $E_{a3D} - E_{a3H} = 1.9 \pm 0.8$ kcal mol^{-1} and $\log(A_{3H}/A_{3D}) = 0.0 \pm 0.5$ values indicate a reaction that falls in region III, where there is extensive tunneling for the H-atom transfer and limited tunneling in the D-transfer reaction. The low A_{3H} and A_{3D} values (both $10^{5.6}$ M^{-1} s^{-1}) are also consistent with tunneling, since they are much lower than the typical bimolecular A values ($10^{8.5}$ to $10^{11.5}$ M^{-1} s^{-1}).[14d]
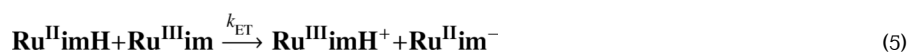
Tunneling has been implicated in a number of metal-mediated HAT reactions and in a few cases the temperature dependence of the isotope effect has been measured. The closest analogy

to reaction 3 are Meyer's reactions of cis-[Ru^{IV}(bpy)$_2$(py)O]$^{2+}$ with H$_2$O$_2$,[42] hydroquinone,[43] and cis-[Ru^{II}(bpy)$_2$(py)(OH$_2$)]$^{2+}$[44] in H$_2$O $vs.$ D$_2$O, which have quite similar KIEs and activation parameters (k_H/k_D = 16.1–28.7 at 298 K; $\Delta H^{\ddagger}_D - \Delta H^{\ddagger}_H$ = 1.5–3.0 kcal mol^{-1}; |$\Delta S^{\ddagger}_H - \Delta S^{\ddagger}_D$| ≤ 2 cal mol^{-1} K^{-1} implying $A_H \approx A_D$) [bpy = 2,2′-bipyridine, py = pyridine]. In contrast, quite different parameters are found for the intramolecular HAT reactions in the decay of Theopold's cobalt μ-peroxo dimer [(Tp″Co)$_2$(μ-O$_2$)][45] and Tolman's μ-oxo copper dimers [(LCu)$_2$(μ-O)$_2$](ClO$_4$)$_2$[46] [Tp″ = hydridotris(3-isopropyl-5-methylpyrazolyl)borate; L = N,N′,N″-R$_3$triazacyclononane, R = CH$_2$Ph, ^{i}Pr]. Both of these reactions have large KIEs and large differences in barriers [($E_{aD} - E_{aH}$)/kcal mol^{-1} = 2.8 (Co), 2.5 and 1.9 (Cu)], and $A_H < A_D$ [A_H/A_D = 0.13 (Co), 0.20 and 0.49 (Cu)], indicating more extensive tunneling for H than for D (region II of the Klinman model).[41] Lipoxygenase enzymes show the unusual combination of temperature independent isotope effects ($E_{aD} - E_{aH}$ close to zero) for reactions with significant activation energies (E_{aH}, $E_{aD} \gg$ 0), which suggests extensive tunneling by both H and D gated by protein motion.[9] There are also many metal-mediated HAT reactions that show modest KIEs.[12a] There is thus a substantial diversity in the tunneling behavior of HAT reactions, and no simple pattern based on structure or driving force is yet evident.

II. Self-Exchange Reaction: Ru^{II}imH(D) + Ru^{III}im

A. Rate and Mechanism—The success of the Marcus cross relation (eq 1) for many HAT reactions has focused attention on degenerate self-exchange HAT reactions (eq 2).[8g,17,47–51] In the adiabatic Marcus picture, the self-exchange reactions carry the intrinsic kinetic information.

For the reaction of **Ru^{II}imH** and **Ru^{III}im**, the observed NMR line broadening could be due to a true HAT self-exchange reaction or could be the result of a stepwise ET-PT or PT-ET reaction, analogous to the discussion above. For such a self-exchange reaction, we have earlier shown that the stepwise ET-PT and PT-ET pathways have the same $\Delta G^{\ddagger}$ and rate constant, based on the principle of microscopic reversibility.[47] For the ET-PT pathway, the rate constant for the initial ET step (eq 5) can be estimated using the Marcus cross relation. This estimate requires the driving force for reaction 5, which is known from the relevant redox potentials,[27] and the ET

$$\textbf{Ru}^{II}\textbf{imH} + \textbf{Ru}^{III}\textbf{im} \xrightarrow{k_{ET}} \textbf{Ru}^{III}\textbf{imH}^+ + \textbf{Ru}^{II}\textbf{im}^- \tag{5}$$

self-exchange rate constant, which is well bracketed by known values for related compounds.[52] Application of the cross relation predicts the rate constant: 5×10^2 M^{-1} s^{-1} < k_{ET} < 4×10^5 M^{-1} s^{-1}.[53] The measured **Ru^{II}imH** + **Ru^{III}im** self-exchange k_{4H} = (3.2 ± 0.3) × 10^5 M^{-1} s^{-1} lies toward the upper limit of the estimated ET rate constant. This means that it is unlikely but not impossible that the self-exchange reaction proceeds by initial ET. Similarly, the H/D isotope effect on the self-exchange rate constant, k_{4H}/k_{4D} = 1.5 ± 0.2 at 298 K, appears to be too large for rate-limiting outer-sphere ET but is not conclusive.

To distinguish between concerted and stepwise mechanisms, the self-exchange rate constant of **Ru^{II}imH** plus **Ru^{III}im** was measured in the less polar solvent THF-d_8, and was found to be an order of magnitude faster than in CD$_3$CN. This is opposite to the expected effect if initial ET or PT were occurring: those paths would generate charged intermediates from the neutral reactants and therefore be less favorable in THF-d_8 than in CD$_3$CN.[54] An HAT path, however, would be expected to be faster in the poorer hydrogen bond accepting solvent THF.[54] Experiments described above also ruled out pathways catalyzed by trace acid (**Ru^{III}imH$^+$**) or base (**Ru^{II}im$^-$**).[55] Thus the evidence, taken all together, indicates a concerted HAT mechanism for self-exchange.

The **Ru^{II}imH** + **Ru^{III}im** self-exchange rate constant $k_{4H} = (3.2 \pm 0.3) \times 10^5$ M^{-1} s^{-1} is close to those for a number of related reactions. HAT self-exchange and pseudo-self-exchange reactions interconverting polypyridyl-ruthenium oxo, hydroxo, and aquo complexes have rate constants from 7.6×10^4 to 7.5×10^5 M^{-1} s^{-1}, the last for a reaction downhill by -2.5 kcal mol^{-1} (Table 2; all self-exchange rate constants are corrected for statistical factors so as to be comparable).[21a,44,56] Iron biimidazoline and bipyrimidine systems have $k_{s.e.}$ values a little slower (by 330 and 180 times) than k_{4H}, both in MeCN at 298 K.[47,48]

Much slower HAT self-exchanges – by many orders of magnitude – have been observed between osmium aniline/anilide complexes,[22] cobalt-biimidazoline complexes[48] and vanadium oxo/hydroxo complexes (Table 2).[21b] The sluggishness of these reactions have been ascribed to large reorganization energies and/or to difficulty in assembly of the HAT precursor complexes, X–H···X. The cobalt reactions, for instance, are most likely slow because they interconvert high-spin Co^{II} and low-spin Co^{III} so that there is a large change in the Co–N bond lengths. The same issue could account for the iron-biimidazoline self-exchange (k_{4H}) being a bit slower than the **Ru^{II}imH** + **Ru^{III}im** reaction reported here: the average difference in Fe–N bond lengths for [Fe^{II}(H$_2$bim)$_3$]$^{2+}$ *vs.* [Fe^{III}(H$_2$bim)$_2$(Hbim)]$^{2+}$ is 0.086(5) Å,[47] while the analogous difference in Ru–O and Ru–N bond lengths is only 0.026(8) Å.[27] On the other hand, the very slow self-exchange in the osmium aniline reaction was suggested to be due to a precursor complex that is disfavored both by sterics and by very weak OsNH···NOs hydrogen bonding.[22] Differences in precursor complex formation could also play a role in comparing reactions of the neutral **Ru^{II}imH** and **Ru^{III}im** species *vs.* the iron complexes. The electrostatic work required to bring two dicationic iron complexes together in MeCN (ionic strength = 0.1) can be estimated to be 1.4 kcal mol^{-1},[47] which would lead to about an order of magnitude slower rate constant.

B. Kinetic Isotope Effects and Tunneling—The ruthenium HAT self-exchange reaction 4 has a small $k_{4H}/k_{4D} = 1.5 \pm 0.2$ at 298 K, which is similar to those found in the iron biimidazoline and bipyrimidine systems (Table 2).[47,48] In the reactions of ruthenium polypyridyl oxo, hydroxo, and aquo complexes, the *pseudo* self-exchange reactions have substantial k_H/k_D values, 5.8–16.1,[44,56] while the KIE for "true" self-exchange is apparently much smaller (Table 2).[21a] As noted above, activation parameters are a more direct probe of tunneling than KIE values. **Ru^{II}imH(D)** + **Ru^{III}im** self-exchange shows substantial $E_{a4D} - E_{a4H} = 1.0 \pm 0.4$ kcal mol^{-1} ($= \Delta H^{\ddagger}_{4D} - \Delta H^{\ddagger}_{4H}$) and negative $\log(A_{4H}/A_{4D}) = -0.5 \pm 0.3$ values, which are perhaps surprising for a reaction with such a small k_{4H}/k_{4D}. The $\log(A_{4H}/A_{4D})$ meets one of Bell's tunneling criteria, $\log(A_H/A_D) < -0.15$,[39] suggesting that hydrogen tunneling plays a role. A_{4H} being a factor of ~3 smaller than A_{4D} suggests that H tunnels more significantly than D (region II of the Klinman model).[41] The ruthenium-oxo reactions with large KIEs also likely involve tunneling, as may the [Fe^{II}(H$_2$bip)$_3$]$^{2+}$ + [Fe^{III}(H$_2$bip)$_2$(Hbip)]$^{2+}$ reaction based on its $\log(A_H/A_D) = 0.9 \pm 1.2$.[48] Tunneling in the iron-biimidazoline and ruthenium-oxo self-exchange reactions has been analyzed in detail by Iordanova, Hammes-Schiffer *et al.* using their multistate continuum model, as is discussed below.[57,58]

III. Applying the Marcus Cross Relation to Ru^{II}imH(D) + TEMPO$^{\bullet}$

The Marcus cross relation has been found to give fairly accurate predictions of HAT rate constants – within one to two orders of magnitude – for a number of systems.[17,18,21] It provides a framework for understanding HAT beyond the traditional Bell-Evans-Polanyi (BEP) correlation of rates with driving force. Unlike the BEP correlation, the cross relation is not limited to comparing similar reactions. However, the generality and limitations of using Marcus approach for HAT are not well understood. The measurements in this study provide a key test of the cross relation, for hydrogen and deuterium atom transfers as a function of temperature, in a system where tunneling is significant.

The calculated Marcus cross rate constant for **Ru^{II}imH(D)** + TEMPO$^\bullet$ ($k_{3,calc}$, eq 6) is derived from the self-exchange rate constants k_4 and TEMPO-H(D)/TEMPO$^\bullet$ (k_7, eq 7),[18,32] the equilibrium constant (K_3), and f.[19,20] Reaction 7 has a large $k_{7H}/k_{7D} = 24 \pm 7$ at 298 K and

$$k_{3,calc} = \sqrt{k_4 k_7 K_3 f} \tag{6}$$
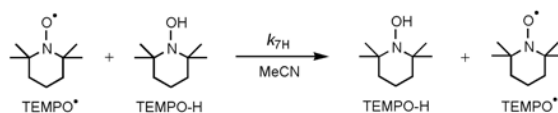
(7)

involves significant hydrogen tunneling (as described elsewhere[32]). The calculated protio and deutero cross rate constants at 298 K are $k_{3H,calc} = (4.3 \pm 0.6) \times 10^4$ M^{-1} s^{-1} and $k_{3D,calc} = (8.4 \pm 1.1) \times 10^3$ M^{-1} s^{-1} (Table 1). Thus, the calculated rate constants for H and D are larger than the observed values by 31 ± 4 and 140 ± 20 times ($= k_{3,calc}/k_3$). These deviations of 1.5 and 2.1 orders of magnitude in applying the Marcus cross relation to HAT reaction 3 are greater than the deviations found for the two iron tris(α-diimine) systems plus TEMPO$^\bullet$/TEMPO-H ($k_{calc}/k_{obs} = 2.9$ and 13).[17]

Activation parameters have been calculated by Eyring analysis (Figure 3b) of the calculated cross rate constants for H and D from 278–318 K using the measured self-exchange rates and equilibrium constants at different temperatures (Table 1).[59] For hydrogen transfer, the calculated $\Delta H^{\ddagger}_{3H,calc}$ of 2.9 ± 0.4 kcal mol^{-1} is in excellent agreement with the observed $\Delta H^{\ddagger}_{3H} = 2.7 \pm 0.5$ kcal mol^{-1}. Thus, the factor of 31 deviation between k_{3H} and $k_{3H,calc}$ is mainly due to the difference in the activation entropies, $\Delta S^{\ddagger}_{3H} - \Delta S^{\ddagger}_{3H,calc} = -7 \pm 4$ cal mol^{-1} K^{-1}. For deuterium, deviations appear to occur in both $\Delta H^{\ddagger}_D$ and $\Delta S^{\ddagger}_D$ terms: $\Delta H^{\ddagger}_{3D} - \Delta H^{\ddagger}_{3D,calc} = 1.0 \pm 0.8$ kcal mol^{-1} and $\Delta S^{\ddagger}_{3D} - \Delta S^{\ddagger}_{3D,calc} = -7 \pm 6$ cal mol^{-1} K^{-1}. Thus, for both the KIE and the activation parameters, the Marcus cross relation gives a better agreement for hydrogen than for deuterium. Interestingly, no effect of isotopic substitution is predicted or observed for the entropies/pre-exponential factors: $\Delta S^{\ddagger}_{3H} = \Delta S^{\ddagger}_{3D}$ and $\log(A_{3H}/A_{3D}) \cong 0$ in both the observed and calculated values.

The Marcus calculated $k_{3H,calc}/k_{3D,calc} = 5.1 \pm 1.0$ at 298 K and $E_{a3D,calc} - E_{a3H,calc} = 0.7 \pm 0.6$ kcal mol^{-1} are within the semi-classical limits,[39] and are smaller than the large observed $k_{3H}/k_{3D} = 23 \pm 3$ and $E_{a3D} - E_{a3H} = 1.9 \pm 0.8$ kcal mol^{-1} values.

The Marcus cross relation was not derived for hydrogen atom transfer, although Marcus discussed it in this context in the 1960s.[60] From one perspective, the cross relation (eqs 1 and 6) can be viewed as little more than an interpolation, one step more sophisticated than a linear free energy relationship (LFER). It averages the kinetic information from the self-exchange rate constants and adjusts them by the overall free energy of reaction. However, the cross relation is more than an extended LFER because all of the parameters can be independently measured and have independent physical meaning. While LFERs are typically limited to a series of quite similar reactions, the cross relation has connected HAT reactions of O–H, N–H and C–H bonds, and connected purely organic and transition metal containing HAT reactions. In reaction 3, for instance, the cross reaction and one of the self-exchange reactions involve ruthenium imidazole/imidazolate complexes while the other self-exchange reaction involves only a nitroxyl and a hydroxylamine.

Recent years have seen much effort in theoretical treatments of reactions such as equation 3, which in this context would be called proton-coupled electron transfer reactions.[25] The most widely discussed approach, Hammes-Schiffer's multistate continuum theory, includes a large number of effects, including the electronic coupling, the Frank-Condon overlaps between reactant and product vibrational wavefunctions in ground and excited states, different reorganization energies for each vibrational transition, and the dependence of most of these parameters on the proton donor-acceptor distance.[12g] None of these are included in the cross relation. In the simple form used here, the cross relation does not explicitly include hydrogen tunneling, the possible non-adiabatic character of the reactions, the involvement of vibrational excited states, or the energetics of forming the precursor complexes. In this light, it is remarkable that the cross relation holds for HAT reactions as well as it does.

The cross relation often holds because of its inherent averaging. This has been discussed for electron transfer reactions that are significantly non-adiabatic or have different energetics for precursor complex formation (w_r).[19] When reactions are non-adiabatic, there is a small probability of crossing from the reactant surface to the product ($\kappa \ll 1$). Even when κ is not explicitly included, the cross relation will hold if κ for the cross reaction is close to the geometric mean of the κ's for the self-exchange reactions. Tunneling presents a similar situation. Taking the simplistic perspective of tunneling as a correction to the transition state theory rate constant, the cross relation should hold when the tunneling contribution to the cross reaction XH + Y is close to the geometric mean of the tunneling contributions to the self-exchange reactions. There is, to our knowledge, no reason why there should be such a relationship among the tunneling contributions. Close adherence to the cross relation should not be expected for reactions in which there is a substantial contribution of tunneling.

In the chemistry described here, hydrogen tunneling is significant for the cross reaction **Ru^{II}imH(D)** + TEMPO$^\bullet$ (eq 3) and for both of the self-exchange reactions (eqs 4 and 7). For all of these reactions, tunneling makes a larger contribution to the rate constant for H than for D. Given that the cross relation does not explicitly include tunneling, one would therefore expect a larger deviation for H-atom transfer than for D-transfer. For reaction 3, however, the agreement with the cross relation is better for H than for D. This suggests that tunneling may not be the primary reason for the 31- and 140-fold deviations observed. Because tunneling corrections are rarely much more than an order of magnitude for reactions near ambient temperatures, the interpolation inherent in the cross relation probably does not introduce errors larger than that order. These deviations observed for reaction 3 could be due to steric, non-adiabatic, and/or hydrogen bonding effects as well as tunneling.

A few words in defense of the cross relation for HAT are warranted. While it is not a sophisticated or by any means a complete treatment, in our view it captures the two most important features of an HAT reaction: the driving force $\Delta G°$ and the reorganization energy.[4] Of all the HAT reactions we have examined, the largest deviation from the cross relation is a factor of about 300. While this is poor agreement for a LFER, it is still better than can typically be done with *ab initio* calculations, particularly for solution reactions with movement of charges, formation of hydrogen bonds, non-adiabatic effects, and significant hydrogen tunneling. In general, to understand the details of a reaction, such as the temperature dependence of the kinetic isotope effect or the influence of protein motions on HAT processes within an active site, the cross relation is not an adequate model. However, if the questions are why a reaction does or does not proceed, or why one reaction is orders of magnitude faster than another, in our view the cross relation proves a very valuable and very accessible approach to the answers.

Conclusions

The reaction of **Ru^{II}imH(D)** + TEMPO$^\bullet$ (eq 3) and the self-exchange reaction **Ru^{II}imH(D)** + **Ru^{III}im** (eq 4) both occur via a concerted HAT mechanism, rather than a stepwise H$^+$/e$^-$ pathway. Reaction 3 involves substantial tunneling as indicated by the large $k_{3H}/k_{3D} = 23 \pm 3$ at 298 K and $E_{a3D} - E_{a3H} = 1.9 \pm 0.8$ kcal mol^{-1}. Tunneling is also important in each of the self-exchange reactions, as indicated by the experimental activation parameters. This is the first system where H and D transfer rates have been measured for both cross and self-exchange reactions over a range of temperatures, allowing a detailed probe of the applicability of the Marcus cross relation. The rate constants for reaction 3 calculated using the cross relation are larger by 31 ± 4 and 140 ± 20 times at 298 K for hydrogen and deuterium, respectively. The cross relation does not predict the large observed k_{3H}/k_{3D}. Application of the cross relation over a range of temperatures gives a calculated $\Delta H^\ddagger_{3H,calc} = 2.9 \pm 0.4$ kcal mol^{-1} for H transfer that is in excellent agreement with the observed $\Delta H^\ddagger_{3H} = 2.7 \pm 0.5$ kcal mol^{-1}; the primary deviation is in the activation entropy ($\Delta S^\ddagger_{3H} - \Delta S^\ddagger_{3H,calc} = -7 \pm 4$ cal mol^{-1} K^{-1}). For deuterium, there appear to be discrepancies in both the $\Delta H^\ddagger_D$ and $\Delta S^\ddagger_D$.

The simple application of the cross relation does not explicitly account for hydrogen tunneling and therefore close agreement should not be expected. The cross relation includes only the driving force and the intrinsic barriers, the latter estimated from the self-exchange rates. The cross relation does have, however, some implicit averaging and even though tunneling is not included, it should hold if the effective tunneling correction for the cross relation is the mean of the corrections for the self-exchange reactions. In the case of **Ru^{II}imH(D)** + TEMPO$^\bullet$ (eq 3), the agreement is better for H transfer than for D despite the greater tunneling for H, suggesting that tunneling is not the primary origin of the discrepancy from the cross relation prediction. While this study better defines the limitations of applying the cross relation to HAT reactions, it also illustrates the value of this approach. The cross relation succeeds as well as it does because if its inherent averaging and because it captures the effects of driving force and intrinsic barrier that are the two largest influences on the rate constant.

Experimental

Physical Techniques and Instrumentation

^{1}H NMR (500 MHz) spectra were recorded on a Bruker Avance spectrometer, referenced to a residual solvent peak. UV-vis spectra were acquired with a Hewlett-Packard 8453 diode array spectrophotometer in anhydrous MeCN, and are reported as λ_{max}/nm (ε/M^{-1} cm^{-1}). UV-vis stopped-flow measurements were obtained on an OLIS RSM-1000 stopped-flow spectrophotometer. IR spectra were obtained as KBr pellets or as CD$_3$CN solution in a NaCl solution cell using a Bruker Vector 33 or Perkin-Elmer 1720 FT-IR spectrometer. All reactions were performed in the absence of air using glove box/vacuum line techniques.

Materials

All reagent grade solvents were purchased from Fisher Scientific, EMD Chemicals, or Honeywell Burdick & Jackson (anhydrous MeCN). MeCN was sparged with Ar and piped from a steel keg directly into a glove box. Deuterated solvents were obtained from Cambridge Isotope Laboratories. CD$_3$CN was dried over CaH$_2$, vacuum transferred to P$_2$O$_5$, then over to CaH$_2$, and then to an empty glass vessel. THF-d_8 was dried over Na/Ph$_2$CO. TEMPO$^\bullet$ (λ_{max} = 460 nm, ε = 10.3 M^{-1} cm^{-1})[18] and Cp$_2$Co were purchased from Aldrich, and were sublimed onto a cold-finger before use. **Ru^{II}imH** (λ_{max} = 568 nm, ε = 7000 M^{-1} cm^{-1}),[27] **Ru^{III}im** (λ_{max} = 486 nm, ε = 1600 M^{-1} cm^{-1}),[27] and TEMPO-H[18,61] were prepared according to literature procedures. TEMPO-D was prepared in 70% yield analogously to TEMPO-H, using

$(CD_3)_2CO/D_2O$ (99.9% D in D_2O) as the solvent. TEMPO-D deuteration was $98 \pm 1\%$, as determined by NMR integration of the residual OH resonance (δ 5.34 in CD_3CN).

The errors on K_3, k_3, k_4, $\Delta H°_3$, $\Delta S°_3$ and the activation parameters are reported as 2σ, derived from the least-squares linear fits (using KaleidaGraph[62]) to plots *vs.* [TEMPO-H(D)] or to the van't Hoff, Eyring, or Arrhenius equations.

$Ru^{III}im$ + TEMPO-H(D) ⇌ $Ru^{II}imH(D)$ + TEMPO• Equilibrium Constant Measurements

Stock solutions of **$Ru^{III}im$** (0.48 mM) and TEMPO-H (240 mM) in MeCN were prepared inside a glove box. An aliquot of **$Ru^{III}im$** (2.5 mL) was transferred to a UV-vis cuvette, which was allowed to thermally equilibrate at 269–310 K. The solution was titrated with TEMPO-H (0.2–7 equiv, 10 μL = 0.2 equiv). UV-vis spectra were recorded for the initial **$Ru^{III}im$,** and after each addition of TEMPO-H when the solution has reached equilibrium. The UV-vis data were analyzed using the absorbance at 568 nm, yielding [**$Ru^{II}imH$**]/[**$Ru^{III}im$**] = (A − A_{RuIII})/(A_{RuII} − A), where A_{RuII} and A_{RuIII} are the absorbances for pure **$Ru^{II}imH$** and **$Ru^{III}im$** at 568 nm (ε = 7000 M^{-1} cm^{-1} for **$Ru^{II}imH$**, 670 M^{-1} cm^{-1} for **$Ru^{III}im$**).[27] By mass balance, [**$Ru^{II}imH$**] = [TEMPO•] = {((A − A_{RuIII})/(A_{RuII} − A_{RuIII})) × [Ru]$_{total}$}, and [TEMPO-H] = [TEMPO-H]$_{total}$ − [TEMPO•] = [TEMPO-H]$_{total}$ − {((A − A_{RuIII})/(A_{RuII} − A_{RuIII})) × [Ru]$_{total}$}. Plotting [**$Ru^{II}imH$**][TEMPO•]/[**$Ru^{III}im$**] *vs.* [TEMPO-H] yielded a straight line, whose slope is the equilibrium constant for the uphill reaction: **$Ru^{III}im$** + TEMPO-H ⇌ **$Ru^{II}imH$** + TEMPO• ($1/K_{3H}$ = (5.5 ± 0.6) × 10^{-4} at 298 K; Figure 1a). The deutero K_{3D} was determined analogously using TEMPO-D in MeCN.

Kinetic Measurements of $Ru^{II}imH(D)$ with TEMPO•

Solutions of **$Ru^{II}imH$** (0.093–0.11 mM) and TEMPO• (1.1–13 mM) in MeCN were prepared and loaded into gas-tight syringes inside a N_2 glovebox. The stopped-flow apparatus was flushed with anhydrous MeCN, and a background spectrum was acquired. The syringes were immediately loaded onto the stopped-flow apparatus to minimize air exposure. The stopped-flow drive syringes were flushed with the reagents, then filled and allowed to thermally equilibrate. The contents of the two syringes were rapidly mixed at equal volume resulting in half of the original concentrations (0.047–0.053 mM **$Ru^{II}imH$** and 0.53–6.7 mM TEMPO•). A minimum of six kinetic runs were performed for each set of concentrations from 282–337 K. Kinetic data were fit to a first order A → B model over the entire spectral region (460–660 nm, Figure 2) using SPECFIT global analysis software.[31] The derived k_{obs} for each TEMPO• concentration was plotted *vs.* [TEMPO•], and the slope of the straight line is the bimolecular rate constant k_{3H} (Figure 3a). The presence of CH_3OH (25 mM) in the reactions of **$Ru^{II}imH$** (0.047–0.053 mM) and TEMPO• (0.53–6.7 mM) from 278–333 K did not affect the same rate constant within error. The deuterium reaction was studied analogously (278–333 K) using syringes loaded with **$Ru^{II}imD$** (0.093–0.11 mM), with 49 mM CD_3OD (99.8% D) as deuteration agent, and TEMPO• (1.1–150 mM).

$Ru^{II}imH(D)/Ru^{III}im$ Self-Exchange Measurements

Stock solutions of **$Ru^{II}imH$** (2.0 mM, 4.5 mg in 5.0 mL) and **$Ru^{III}im$** (9.2 mM, 4.1 mg in 1.0 mL) in CD_3CN were prepared inside a N_2 glove box. Each of seven J-Young NMR tubes was loaded with **$Ru^{II}imH$** solutions (0.5 mL), and 5–30 μL of **$Ru^{III}im$** solutions were added to six tubes to give **$Ru^{III}im$** concentrations of 0.092–0.73 mM, with one tube containing a solution of only **$Ru^{II}imH$**. ^{1}H NMR spectra were obtained at 250–363 K for each tube. The CH_3-acac resonance (δ 1.51; initial fwhm = 2–4 Hz) of **$Ru^{II}imH$** was Lorentzian line fitted using NUTS software[34] to determine the line width (fwhm) in each sample. Plotting π(Δfwhm) *vs.* [**$Ru^{III}im$**] yielded a straight line, where Δfwhm = [fwhm(**$Ru^{II}imH$**/**$Ru^{III}im$**) − fwhm (**$Ru^{II}imH$**)], and the slope is the self-exchange rate constant k_{4H} (Figure 5a). Experiments with **$Ru^{II}imH$** (2.0 mM) with **$Ru^{III}im$** (0.10–0.59 mM) in the presence of CH_3OH (250 mM) in

CD_3CN gave the same rate constant within error from 250–363 K. The deutero rate constant, k_{4D} was measured similarly using **Ru^{II}imD** (2.0 mM) and **Ru^{III}im** (0.089–0.59 mM) in the presence of CD_3OD (250 mM) in CD_3CN at 250–363 K. The same procedure, line fitting the δ1.48 CH_3-acac resonance, was used to measure k_{4H} in THF-d_8 at 298 K for the reaction of **Ru^{II}imH** (2.0 mM) [with and without pre-treatment with 0.011 mM Cp_2Co] and **Ru^{III}im** (0.011–0.16 mM).

Acknowledgements

References

1. Hynes, JT.; Klinman, JP.; Limbach, H-H.; Schowen, RL., editors. Hydrogen-Transfer Reactions. Wiley-VCH; Weinheim: 2007.

2. Olah, GA.; Molnár, Á. Hydrocarbon Chemistry. Vol. 2. Wiley; Hoboken, NJ: 2003. Sheldon, RA.; Kochi, JK. Metal-Catalyzed Oxidations of Organic Compounds. Academic Press; New York: 1981. Kochi, JK. Free Radicals. Wiley; New York: 1973. Halliwell, B.; Gutteridge, JMC. Free Radicals in Biology and Medicine. Oxford University Press; Oxford: 1999. Fossey, J.; Lefort, D.; Sorba, J. Free Radicals in Organic Chemistry. Wiley; New York: 1995. Lazár, M.; Rychlý, J.; Klimo, V.; Pelikán, P.; Valko, L. Free Radicals in Chemistry and Biology. CRC Press; Boca Raton, Fl: 1989.

3. For recent references, see (a) Gansäuer A, Fan CA, Piestert F. J Am Chem Soc 2008;130:6916. [PubMed: 18457391] (b) Nieto I, Ding F, Bontchev RP, Wang H, Smith JM. J Am Chem Soc 2008;130:2716. [PubMed: 18266366] (c) Maiti D, Lee D-H, Gaoutchenova K, Würtele C, Holthausen MC, Narducci Sarjeant AA, Sundermeyer J, Schindler S, Karlin KD. Angew Chem Int Ed 2008;47:82. (d) Lam WWY, Man WL, Leung CF, Wong CY, Lau TC. J Am Chem Soc 2007;129:13646. [PubMed: 17929922] (e) Zdilla MJ, Dexheimer JL, Abu-Omar MM. J Am Chem Soc 2007;129:11505. [PubMed: 17718564] (f) Choi J, Tang L, Norton JR. J Am Chem Soc 2007;129:234. [PubMed: 17199304] (g) Vasbinder MJ, Bakac A. Inorg Chem 2007;46:2921. [PubMed: 17290988] (h) Zhang J, Grills DC, Huang KW, Fujita E, Bullock RM. J Am Chem Soc 2005;127:15684. [PubMed: 16277493]

4. (a) Mayer JM. Annu Rev Phys Chem 2004;55:363. [PubMed: 15117257] (b) Mayer JM, Rhile IJ. Biochim Biophys Acta 2004;1655:51. [PubMed: 15100016] (c) Mayer JM, Rhile IJ, Larsen FB, Mader EA, Markle TF, DiPasquale AG. Photosynth Res 2006;87:3. [PubMed: 16437185] (d) Mayer JM, Mader EA, Roth JP, Bryant JR, Matsuo T, Dehestani A, Bales BC, Watson EJ, Osako T, Valliant-Saunders K, Lam W-H, Hrovat DA, Borden WT, Davidson ER. J Mol Catal A: Chem 2006;251:24. (e) Isborn C, Hrovat DA, Borden WT, Mayer JM, Carpenter BK. J Am Chem Soc 2005;127:5794. [PubMed: 15839670]

5. Warren JJ, Mayer JM. J Am Chem Soc 2008;130:2774–2776. [PubMed: 18257574]

6. Manner VW, DiPasquale AG, Mayer JM. J Am Chem Soc 2008;130:7210–7211. [PubMed: 18479096]

7. (a) Hernández-García L, Quintero L, Sánchez M, Sartillo-Piscil F. J Org Chem 2007;72:8196. [PubMed: 17900138] (b) Hartung J. Eur J Org Chem 2001:619. (c) Lucarini M, Pedrielli P, Pedulli GF, Valgimigli L, Gigmes D, Tordo P. J Am Chem Soc 1999;121:11546.

8. (a) Sheldon RA, Arends IWCE. J Mol Catal A: Chem 2006;251:200. (b) Sheldon RA, Arends IWCE. Adv Synth Catal 2004;346:1051. (c) Sheldon RA, Arends IWCE, Brink GJT, Dijksman A. Acc Chem Res 2002;35:774. [PubMed: 12234207] (d) Ishii Y, Sakaguchi S, Iwahama T. Adv Synth Catal 2001;343:393. (e) Koshino N, Saha B, Espenson JH. J Org Chem 2003;68:9364. [PubMed: 14629158] (f) Koshino N, Cai Y, Espenson JH. J Phys Chem A 2003;107:4262. (g) Cai Y, Koshino N, Saha B, Espenson JH. J Org Chem 2005;70:238. [PubMed: 15624928] (h) Amorati R, Lucarini M, Mugnaini V, Pedulli GF. J Org Chem 2003;68:1747. [PubMed: 12608787] (i) Barreca AM, Sjögren B, Fabbrini M, Galli C, Gentili P. Biocatal Biotransform 2004;22:105.

9. (a) Knapp MJ, Meyer M, Klinman JP. 4:1241–1284.In ref. 1 (b) Knapp MJ, Rickert K, Klinman JP. J Am Chem Soc 2002;124:3865. [PubMed: 11942823] (c) Lewis ER, Johansen E, Holman TR. J Am Chem Soc 1999;121:1395.

10. (a) Mayer JM. Acc Chem Res 1998;31:441. (b) Gardner KA, Mayer JM. Science 1995;269:1849. [PubMed: 7569922]

11. Partenheimer W. Catal Today 1995;23:69.

12. (a) Huynh MHV, Meyer TJ. Chem Rev 2007;107:5004. [PubMed: 17999556] (b) Fecenko CJ, Thorp HH, Meyer TJ. J Am Chem Soc 2007;129:15098. [PubMed: 17999500] (c) Meyer TJ, Huynh MHV. Inorg Chem 2003;42 (d) Hodgkiss JM, Rosenthal J, Nocera DG. 2:503–562.In ref. 1 (e) Stubbe J, Nocera DG, Yee CS, Chang MCY. Chem Rev 2003;103:2167. [PubMed: 12797828] (f) Cukier RI, Nocera DG. Annu Rev Phys Chem 1998;49:337. [PubMed: 9933908] (g) Hammes-Schiffer S. 2:479–502.In ref. 1 (h) Irebo T, Reece SY, Sjödin M, Nocera DG, Hammarström L. J Am Chem Soc 2007;129:15462. [PubMed: 18027937] (i) Lomoth R, Magnuson A, Sjödin M, Huang P, Styring S, Hammarström L. Photosynth Res 2006;87:25. [PubMed: 16416050] (j) Costentin C, Robert M, Savéant JM. J Am Chem Soc 2007;129:9953. [PubMed: 17637055]

13. (a) Markle TF, Rhile IJ, DiPasquale AG, Mayer JM. Proc Nat Acad Sci USA 2008;105:8185–8190. [PubMed: 18212121] (b) Markle TF, Mayer JM. Angew Chem Int Ed 2008;47:738. (c) Rhile IJ, Markle TF, Nagao H, DiPasquale AG, Lam OP, Lockwood MA, Rotter K, Mayer JM. J Am Chem Soc 2006;128:6075. [PubMed: 16669677] (d) Rhile IJ, Mayer JM. J Am Chem Soc 2004;126:12718. [PubMed: 15469234] (e) Lingwood M, Hammond JR, Hrovat DA, Mayer JM, Borden WT. J Chem Theory Comput 2006;2:740. [PubMed: 18725967] (f) Mayer JM, Hrovat DA, Thomas JL, Borden WT. J Am Chem Soc 2002;124:11142. [PubMed: 12224962]

14. (a) Tishchenko O, Truhlar DG, Ceulemans A, Nguyen MT. J Am Chem Soc 2008;130:7000. [PubMed: 18465862] (b) Neta P, Grodkowski J. J Phys Chem Ref Data 2005;34:109. (c) Nielsen MF, Ingold KU. J Am Chem Soc 2006;128:1172. [PubMed: 16433533] (d) Foti M, Ingold KU, Lusztyk J. J Am Chem Soc 1994;116:9440. (e) Skone JH, Soudackov AV, Hammes-Schiffer S. J Am Chem Soc 2006;128:16655. [PubMed: 17177415]

15. Ingold, KU. Free Radicals. Kochi, JK., editor. Vol. Chapter 2. Wiley; New York: 1973. p. 69ffRussell, GA. Free Radicals. Kochi, JK., editor. Vol. Chapter 7. Wiley; New York: 1973. p. 283-293. (b) Tedder JM. Angew Chem, Int Ed Engl 1982;21:401.

16. Mader EA, Davidson ER, Mayer JM. J Am Chem Soc 2007;129:5153. [PubMed: 17402735]

17. Roth JP, Yoder JC, Won TJ, Mayer JM. Science 2001;294:2524. [PubMed: 11752572]

18. Mader EA, Larsen AS, Mayer JM. J Am Chem Soc 2004;126:8066. [PubMed: 15225018]

19. (a) Marcus RA, Sutin N. Biochim Biophys Acta 1985;811:265. (b) Sutin N. Prog Inorg Chem 1983;30:441.

20. $f_{XY} = \exp[(\ln(K_{XY}))^2/(4\ln(k_{XX}k_{YY}/Z^2))]$, where the collision frequency, $Z \approx 10^{11}$ M^{-1} s^{-1}.[19]

21. (a) Bryant JR, Mayer JM. J Am Chem Soc 2003;125:10351–10361. [PubMed: 12926960] (b) Waidmann CR, Zhou X, Kaminsky W, Hrovat DA, Borden WT, Mayer JM. manuscript in preparation

22. Soper JD, Mayer JM. J Am Chem Soc 2003;125:12217. [PubMed: 14519007]

23. Manner, V. W.; Lindsay, A.; Mayer, J. M., work in progress.

24. Goldsmith CR, Jonas RT, Stack TDP. J Am Chem Soc 2002;124:83–96. [PubMed: 11772065]

25. (a) Refs. 1, 12, and 14a. (b) Hammes-Schiffer S, Hatcher E, Ishikita H, Skone JH, Soudackov AV. Coord Chem Rev 2008;252:384–394. (c) Marcus RA. Phil Trans R Soc Lond B Biol Sci 2006;361:1445–1455. [PubMed: 16873131] (d) Cukier RI. J Phys Chem B 2002;106:1746–1757. (d) Kotelnikov AI, Medvedev ES, Medvedev DM, Stuchebrukhov AA. J Phys Chem B 2001;105:5789–5796.

26. cf., (a) Ref. 12b. (b) Hodgkiss JM, Damrauer NH, Presse S, Rosenthal J, Nocera DG. J Phys Chem B 2006;110:18853–18858. [PubMed: 16986876]

27. Wu A, Masland J, Swartz RD, Kaminsky W, Mayer JM. Inorg Chem 2007;46:11190. [PubMed: 18052056]

28. Bell, RP. The Proton in Chemistry. Vol. 2. Cornell University Press; Ithaca, NY: 1973. p. 226-296.

29. $K_H/K_D = \exp[hc((\nu_{NH} - \nu_{ND}) - (\nu_{OH} - \nu_{OD}))/2k_BT] = 0.78$, where T = 298 K, $\nu_{NH} = 3068$ cm^{-1} and $\nu_{ND} = 2267$ cm^{-1} for Ru^{II}imH(D) in KBr pellets, and $\nu_{OH} = 3495$ cm^{-1} and $\nu_{OD} = 2592$ cm^{-1} for TEMPO-H(D) in CD_3CN.

30. Mader EA, Manner VW, Wu A, Mayer JM. manuscript in preparation

31. SPECFIT/32, versions v3.0.26 and v3.0.36. Spectrum Software Associates; Marlborough, MA: 2000.

32. Wu A, Datta A, Mader EA, Hrovat DA, Borden WT, Mayer JM. to be submitted

33. Sandström, J. Dynamic NMR Spectroscopy. Academic Press; London: 1982.

34. NUTS − NMR Utility Transform Software, 1D version. Acorn NMR Inc.; Livermore, CA: 2003.

35. The singlet at δ 1.51 corresponds to two accidentally degenerate methyl groups. This peak remained degenerate and unobscured throughout the entire measured temperature range (250–363 K), and was suitable for line broadening analysis by NUTS software. The other two methyl singlets (δ 2.00, 2.05) were obscured by the residual solvent pentet at δ 1.94 (CD$_2$HCN), and were not suitable for line fitting. The two overlapping CH-acac singlets (δ 5.29, 5.32) and other non-singlet aromatic resonances were unable to be line fitted by NUTS, but instead using gNMR software.

36. gNMR software, v4.1.0. Ivory Soft; Rancho Palos Verdes, CA: 1999.

37. (a) $\Delta G°(ET) = -23.1[E(TEMPO^•) - E(Ru^{II}imH)] = +29$ kcal mol^{-1}; $\Delta G°(PT) = -1.37[pK_a(TEMPO-H^{•+}) - pK_a(Ru^{II}imH)] = +34$ kcal mol^{-1}; $\Delta G°(HAT) = -4.4$ kcal mol^{-1} from $K_{3H} = 1.8 \times 10^3$. (b) $E(Ru^{II}imH) = -0.64$ V vs. Cp$_2$Fe$^{+/0}$, pK$_a$(Ru^{II}imH) = 22.1: ref. 27. (c) $E(TEMPO^•) \approx -1.91$ V vs. Cp$_2$Fe$^{+/0}$: Mori Y, Sakaguchi Y, Hayashi H. J Phys Chem A 2000;104:4896.(d) pK$_a$(TEMPO-H$^{•+}$) = pK$_a$(TEMPO-H) + 23.1[E(TEMPO•) − E(TEMPO-H)]/1.37 ≈ −3. (e) E(TEMPO-H) ≈ 0.71 V vs. Cp$_2$Fe$^{+/0}$: Semmelhack MF, Chou CS, Cortes DA. J Am Chem Soc 1983;105:4492.(f) pK$_a$(TEMPO-H) ≈ 41 in MeCN is estimated from pK$_a$(TEMPO-H) = 31.0 in DMSO: Bordwell FG, Liu WZ. J Am Chem Soc 1996;118:10819.(g) pK$_a$ conversion from DMSO to MeCN: Chantooni MK Jr, Kolthoff IM. J Phys Chem 1976;80:1306.

38. (a) Njus D, Kelley PM. FEBS Lett 1991;284:147–151. [PubMed: 1647978] (b) Vuina D, Pilepic V, Ljubas D, Sankovic K, Sajenko I, Uršic S. Tet Lett 2007;48:3633–3637.

39. Bell, RP. The Tunnel Effect in Chemistry. Chapman and Hall; London: 1980. p. 77-105.

40. Semi-classical $k_H/k_D = \exp[hc(\nu_{NH} - \nu_{ND})/2k_BT] = 6.9$, where T = 298 K.

41. (a) Klinman JP. Phil Trans R Soc B 2006;361:1323. [PubMed: 16873120] (b) Kohen A, Klinman JP. Acc Chem Res 1998;31:397. (c) Jonsson T, Glickman MH, Sun S, Klinman JP. J Am Chem Soc 1996;118:10319.

42. (a) Gilbert JA, Gersten SW, Meyer TJ. J Am Chem Soc 1982;104:6872. (b) Gilbert J, Roecker L, Meyer TJ. Inorg Chem 1987;26:1126.

43. Binstead RA, McGuire ME, Dovletoglou A, Seok WK, Roecker LE, Meyer TJ. J Am Chem Soc 1992;114:173.

44. Binstead RA, Meyer TJ. J Am Chem Soc 1987;109:3287.

45. Reinaud OM, Theopold KH. J Am Chem Soc 1994;116:6979.

46. Mahapatra S, Halfen JA, Tolman WB. J Am Chem Soc 1996;118:11575.[(LCu)$_2$(μ-O)$_2$](ClO$_4$)$_2$ with L = 1,4,7-tribenzyl-7-benzyl-1,4,7-triazacyclononane or 1,4,7-triisopropyl-7-benzyl-1,4,7-triazacyclononane.

47. Roth JP, Lovell S, Mayer JM. J Am Chem Soc 2000;122:5486.

48. Yoder JC, Roth JP, Gussenhoven EM, Larsen AS, Mayer JM. J Am Chem Soc 2003;125:2629. [PubMed: 12603151]

49. Kiss G, Zhang K, Mukerjee SL, Hoff CD. J Am Chem Soc 1990;112:5657.The CpCr(CO)$_3$H + CpCr(CO)$_3$• self-exchange rate constant k ~ 10^2 M^{-1} s^{-1} is estimated from k = 910 M^{-1} s^{-1} at 298 K for CpCr(PPh$_3$)(CO)$_2$H + (C$_5$Me$_5$)Cr(CO)$_3$• in toluene ($\Delta H° = -2.5$ kcal mol^{-1}).

50. Protasiewicz JD, Theopold KH. J Am Chem Soc 1993;115:5559.

51. Song J, Bullock RM, Creutz C. J Am Chem Soc 1991;113:9862.

52. The self-exchange rate constant for Ru^{II}imH + Ru^{III}imH$^+$ is estimated to be between 4×10^6 and 1×10^8 M^{-1} s^{-1} in MeCN based on the following k(self-exchange) values: (a) 1.4×10^8 M^{-1} s^{-1} for [Ru(acac)$_2$(4,4′-Me$_2$bpy)]$^{0/+}$, 4.5×10^6 M^{-1} s^{-1} for [Ru(hfac)$_2$(4,4′-Me$_2$bpy)]$^{0/+}$, 5.0×10^6 M^{-1} s^{-1} for [Ru(hfac)$_3$]$^{-/0}$, 8.3×10^6 M^{-1} s^{-1} for [Ru(bpy)$_3$]$^{2+/3+}$, and 1×10^8 M^{-1} s^{-1} for [Ru(L)$_3$]$^{2+/3+}$ (L = 3,4,7,8-Me$_4$phen, 3,5,6,8-Me$_4$phen, or 4,7-Me$_2$bpy) [hfac = 1,1,1,5,5,5-hexafluoro-2,4-pentanedionato, phen = 1,10-phenanthroline]. (b) Wherland S. Coord Chem Rev 1993;123:169. (c) Chan MS, Wahl AC. J Phys Chem 1982;86:126.

53. (a) The range of rate constants from footnote 52, using $k = Ze^{-\Delta G*/RT}$ and a collision frequency Z of 10^{11} M^{-1} s^{-1} gives $\Delta G* = 5.0 \pm 1.0$ kcal mol^{-1}.[19] From the (adiabatic) Marcus equation, $\Delta G* = w_r + (\lambda/4)(1 + \Delta G°'/\lambda)^2$, the intrinsic barrier $\lambda_{ET} = 4\Delta G* = 20 \pm 4$ kcal mol^{-1} (the work term $w_r = 0$).[19] Reaction 5 has $\Delta E_{1/2} = -0.36$ V[27] or $\Delta G° = +8.3$ kcal mol^{-1}. After correcting for the

electrostatic effects,[53b] $\Delta G^{\circ\prime} = 7.3$ kcal mol^{-1}. Inserting this value and the λ_{ET} above into the Marcus equation above gives $\Delta G^* = 9.3 \pm 2.0$ kcal mol^{-1} which (using $Z = 10^{11}$ M^{-1} s^{-1}) gives $5 \times 10^2 < k_{ET} < 4 \times 10^5$ M^{-1} s^{-1}. EbersonLElectron Transfer Reactions in Organic ChemistrySpringer-VerlagBerlin19872728

54. Litwinienko G, Ingold KU. Acc Chem Res 2007;40:222. [PubMed: 17370994]

55. Cf., Refs. 22, 54, and Soper JD, Rhile IJ, DiPasquale AG, Mayer JM. Polyhedron 2004;23:323.

56. Farrer BT, Thorp HH. Inorg Chem 1999;38:2497.

57. Iordanova N, Hammes-Schiffer S. J Am Chem Soc 2002;124:4848. [PubMed: 11971735]

58. Iordanova N, Decornez H, Hammes-Schiffer S. J Am Chem Soc 2001;123:3723. [PubMed: 11457104]

59. The Eyring parameters, $\Delta H^{\ddagger}_{3,\text{calc}}$ and $\Delta S^{\ddagger}_{3,\text{calc}}$ were determined from $k_{3,\text{calc}}$ values, which were calculated from the k_4, k_8, and K_3 terms at different temperatures derived from their respective Eyring or van't Hoff equation.

60. (a) Marcus RA. J Phys Chem 1968;72:891–899.See also: (b) Albery WJ. Faraday Disc Chem Soc 1982;74:245–256.and ref. 25c

61. Ozinskas AJ, Bobst AM. Helv Chim Acta 1980;63:1407.
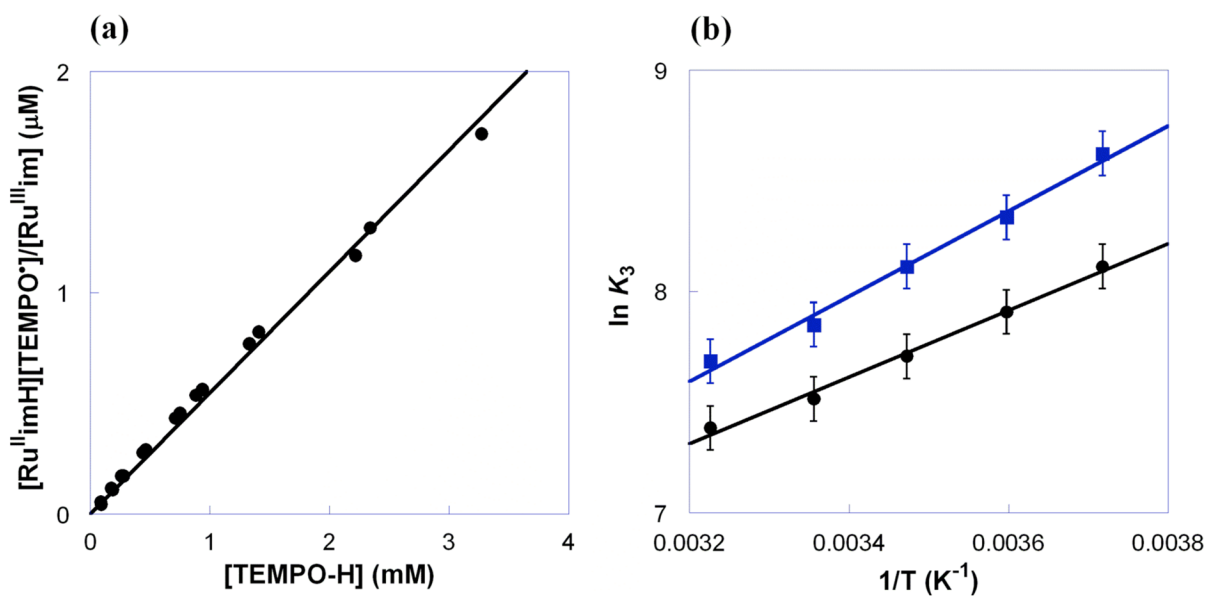
62. KaleidaGraph, version 3.5; Synergy Software: 2000.

Figure 1.
(a) Plot of [**Ru^{II}imH**][TEMPO$^{\bullet}$]/[**Ru^{III}im**] *vs.* [TEMPO-H], with the slope $1/K_{3H} = (5.5 \pm 0.6) \times 10^{-4}$ at 298 K and (b) van't Hoff plot for **Ru^{II}imH(D)** + TEMPO$^{\bullet}$ $\rightleftharpoons$ **Ru^{III}im** + TEMPO-H(D) ($K_{3H} = \bullet$, $K_{3D} = \blacksquare$) in MeCN.
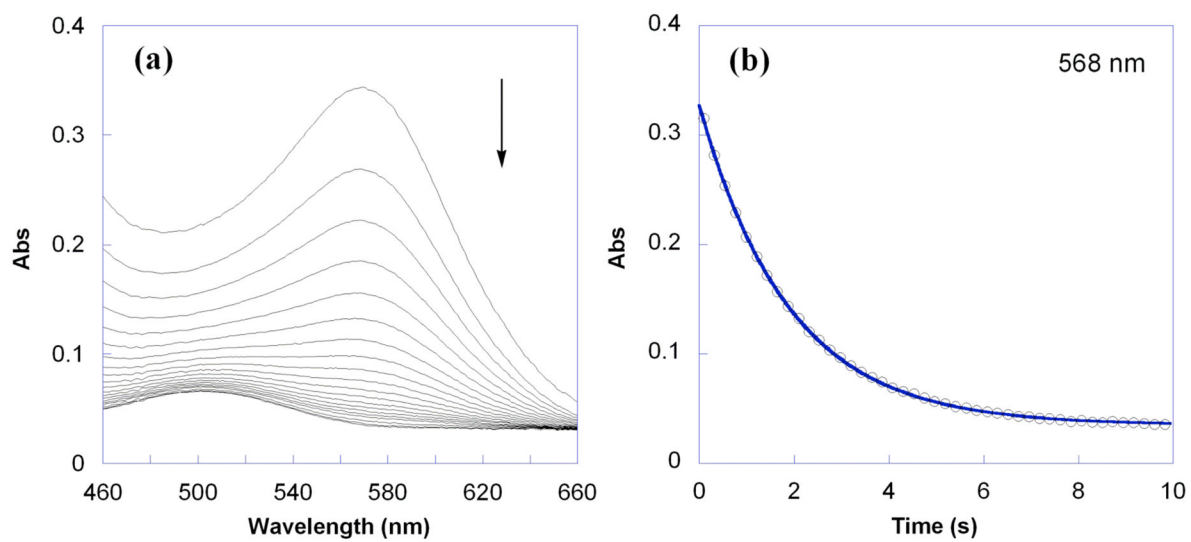
Figure 2.
(a) Overlay of UV-vis spectra for the reaction of **Ru^{II}imH** (0.053 mM) with TEMPO$^{\bullet}$ (0.53 mM) in MeCN at 298 K over 10 s. (b) Absorbance at 568 nm showing the raw data (○) and first order A → B fit using SPECFIT (—).
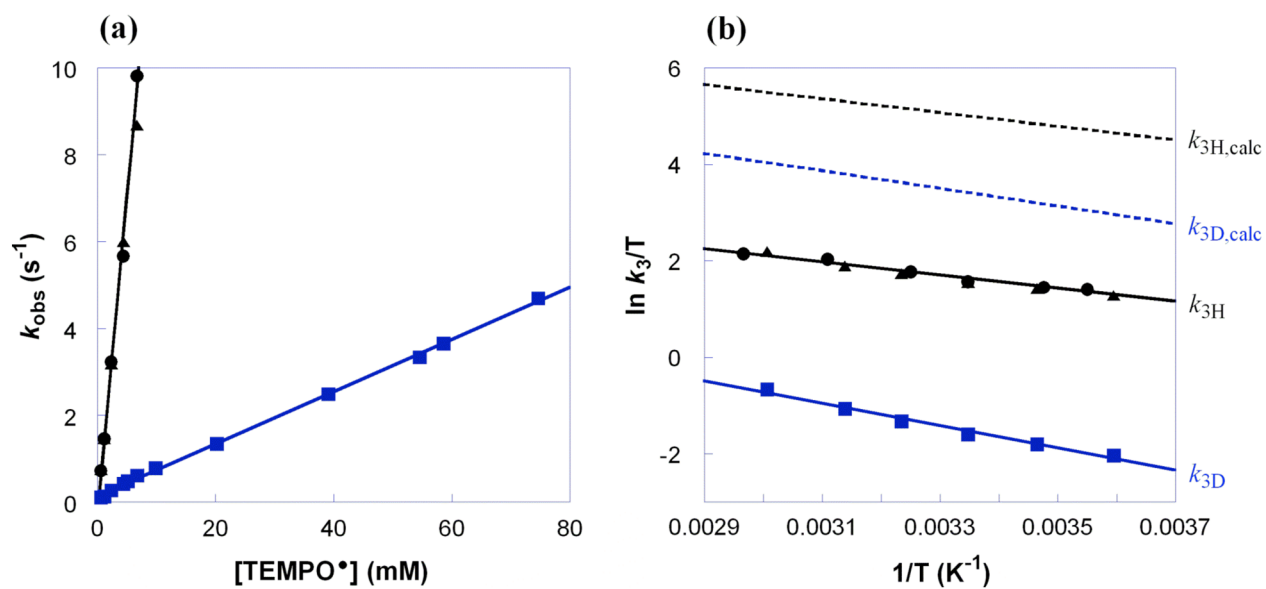
Figure 3.
(a) Pseudo first order plot of k_{obs} *vs.* [TEMPO$^\bullet$] at 298 K and (b) Eyring plot for the reactions of **Ru^{II}imH(D)** with TEMPO$^\bullet$ in MeCN [k_{3H} = $\bullet$ (no CH$_3$OH), $\blacktriangle$ (25 mM CH$_3$OH); k_{3D} = $\blacksquare$ (25 mM CD$_3$OD)]. The Eyring plot also shows the calculated $k_{3H,calc}$ and $k_{3D,calc}$ values in dashed lines (---) using the Marcus cross relation (see below).
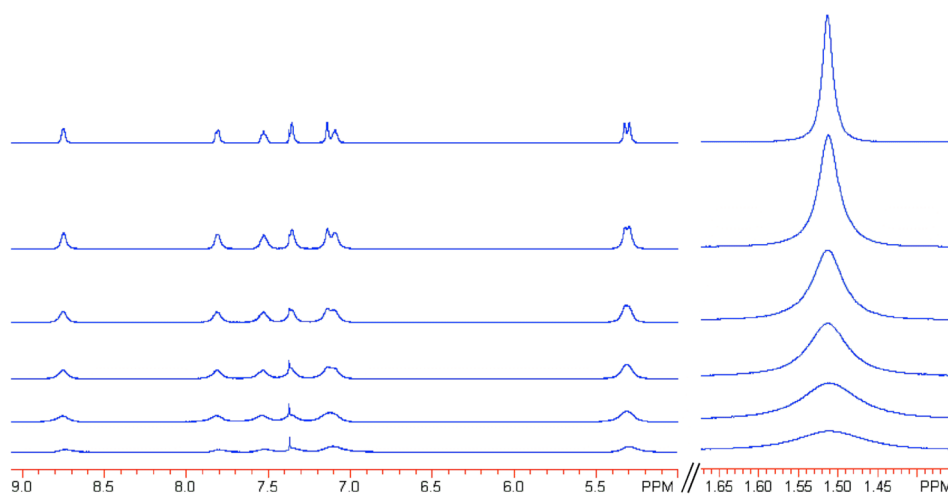
Figure 4.
Partial ^{1}H NMR spectra of **Ru^{II}imH** (2.0 mM, top spectrum) in CD$_3$CN at 298 K, showing line broadening with increasing concentrations of **Ru^{III}im** (0.092–0.73 mM).
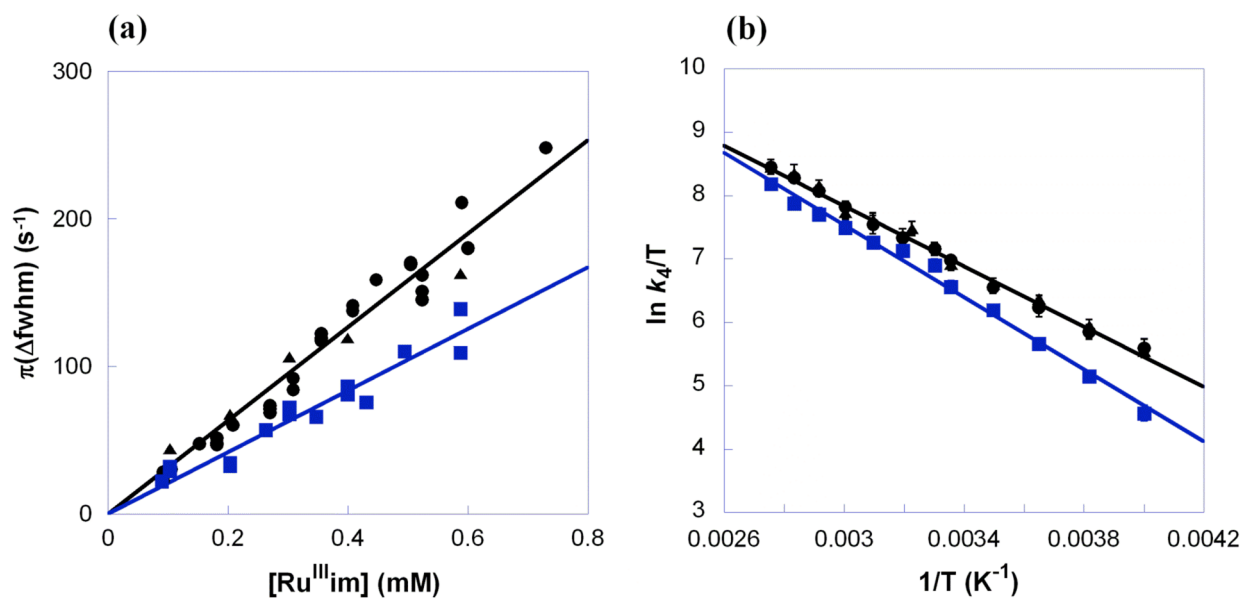
Figure 5.
(a) Plot of $\pi(\Delta\text{fwhm})$ *vs.* [**Ru^{III}im**] at 298 K and (b) Eyring plot for the self-exchange reactions of **Ru^{II}imH(D)** with **Ru^{III}im** in CD$_3$CN [k_{4H} = ● (no CH$_3$OH), ▲ (250 mM CH$_3$OH); k_{4D} = ■ (250 mM CD$_3$OD)].

$$\text{Ru}^{\text{II}}\text{imH} + \text{TEMPO}^{\bullet} \quad \begin{array}{l} \xrightarrow{\text{ET}} \quad \text{Ru}^{\text{III}}\text{imH}^{+} + \text{TEMPO}^{-} \\[1ex] \xrightarrow{\text{PT}} \quad \text{Ru}^{\text{II}}\text{im}^{-} + \text{TEMPO-H}^{+\bullet} \\[1ex] \xrightarrow{\text{HAT}} \quad \text{Ru}^{\text{III}}\text{im} + \text{TEMPO-H} \end{array}$$

(kcal mol^{-1})
+29
+34
-4.4

Chart 1.
Ground state free energy changes for possible initial steps in reaction 3.

Table 1

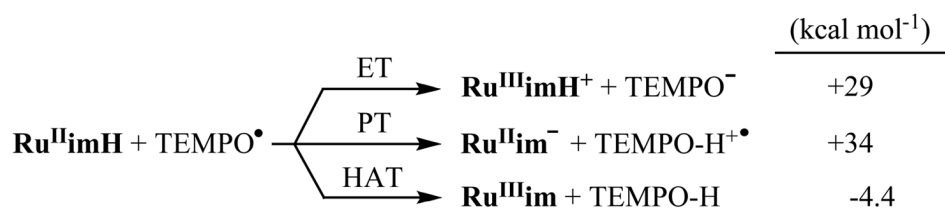Rate Constants, Eyring and Arrhenius Parameters for H- and D-Atom Transfer Reactions.[a]

Reaction	k (M^{-1} s^{-1})	$\Delta H^{\ddagger b}$	$\Delta S^{\ddagger c}$	$E_a^{\ b}$	log A
Ru^{II}imH + TEMPO$^\bullet$	$(1.4 \pm 0.1) \times 10^3$	2.7 ± 0.5	-35 ± 4	3.3 ± 0.5	5.6 ± 0.3
Ru^{II}imD + TEMPO$^\bullet$	60 ± 7	4.6 ± 0.6	-35 ± 5	5.2 ± 0.6	5.6 ± 0.4
Ru^{II}imH + TEMPO$^\bullet$ (calc)[d]	$(4.3 \pm 0.6) \times 10^4$	2.9 ± 0.4	-28 ± 2	3.5 ± 0.4	7.0 ± 0.2
Ru^{II}imD + TEMPO$^\bullet$ (calc)[d]	$(8.4 \pm 1.1) \times 10^3$	3.6 ± 0.5	-28 ± 3	4.2 ± 0.5	7.0 ± 0.3
Ru^{II}imH + **Ru^{III}im**	$(3.2 \pm 0.3) \times 10^5$	4.7 ± 0.2	-17.4 ± 0.4	5.3 ± 0.2	9.4 ± 0.2
Ru^{II}imD + **Ru^{III}im**	$(2.1 \pm 0.2) \times 10^5$	5.7 ± 0.3	-15.3 ± 0.5	6.3 ± 0.2	9.9 ± 0.2
TEMPO$^\bullet$ + TEMPO-H[e]	4.7 ± 1.0	3.8 ± 0.4	-43 ± 2	4.4 ± 0.4	3.8 ± 0.2
TEMPO$^\bullet$ + TEMPO-D[e]	0.20 ± 0.04	5.1 ± 0.4	-44 ± 2	5.7 ± 0.4	3.5 ± 0.2

[a] In MeCN at 298 K.

[b] kcal mol^{-1}.

[c] cal mol K^{-1}.

[d] Calculated from the Marcus cross relation.

[e] Refs. 18 and 32.

Table 2

Self-Exchange and Pseudo Self-Exchange HAT Rate Constants and Deuterium Kinetic Isotope Effects for Transition Metal Coordination Complexes.[a]

Reaction	ΔG° [b]	k_H (M^{-1} s^{-1}) per $H^\bullet$	k_H/k_D	Reference
$Ru^{II}imH$ + **$Ru^{III}im$** [c]	0	$(3.2 \pm 0.3) \times 10^5$	1.5 ± 0.2	this work
$[Fe^{II}(H_2bim)_3]^{2+}$ + $[Fe^{III}(H_2bim)_2(Hbim)]^{2+}$ [c]	0	$(9.7 \pm 0.1) \times 10^2$	2.4 ± 0.3 [d]	47
$[Fe^{II}(H_2bip)_3]^{2+}$ + $[Fe^{III}(H_2bip)_2(Hbip)]^{2+}$ [c]	0	$(1.8 \pm 0.3) \times 10^3$	1.6 ± 0.5	48
$[Ru^{III}(bpy)_2(py)(OH)]^{2+}$ + $[Ru^{IV}(bpy)_2(py)O]^{2+}$ [e]	0	$(7.6 \pm 0.4) \times 10^4$	1.2 ± 0.1	21a
$[Ru^{II}(bpy)_2(py)(OH_2)]^{2+}$ + $[Ru^{IV}(bpy)_2(py)O]^{2+}$ [e]	−2.5	$(1.09 \pm 0.02) \times 10^5$	16.1 ± 0.2	44
$[Ru^{II}(tpy)(bpy)(OH_2)]^{2+}$ + $[Ru^{IV}(tpy)(bpy)O]^{2+}$ [e,f]	−2.5	$(7.45 \pm 0.55) \times 10^5$	11.4 ± 1.3	56
$[Ru^{II}(bpy)_2(py)(OH_2)]^{2+}$ + $[Ru^{III}(tpy)(bpy)(OH)]^{2+}$ [e]	−1.3	$(2.1 \pm 0.1) \times 10^5$	5.8 ± 0.4	44
$TpCl_2Os^{III}(NH_2Ph)$ + $TpCl_2Os^{IV}(NHPh)$ [c,g]	0	$(1.5 \pm 1.0) \times 10^{-3}$	ND	22
$[V^{IV}(4,4'-Me_2bpy)_2(O)(OH)]^+$ + $[V^V(4,4'-{}^tBu_2bpy)_2(O)_2]^+$ [c]	~0	$(6.5 \pm 0.5) \times 10^{-3}$	ND	21b

[a] At 298 K.

[b] kcal mol^{-1}.

[c] In MeCN.

[d] At 324 K.

[e] In H_2O/D_2O; tpy = 2,2′:6′,2″-terpyridine.

[f] Other analogous Ru(H$_2$O)/Ru(O) reactions, not shown in Table 2, have k_H = 2.1×10^5 to 1.5×10^6 M^{-1} s^{-1} per $H^\bullet$ and k_H/k_D = 9.8–12.3 at 298 K. 56

[g] Tp = hydrotris(pyrazolyl)borate.